Network MIMO Downlink Transmission

Clemens Stierstorfer, Christian Siegl, Robert F.H. Fischer
Lehrstuhl für Informationsübertragung
Friedrich-Alexander-Universität Erlangen-Nürnberg
Cauerstraße 7/LIT, 91058 Erlangen, Germany
Email:{clemens,siegl,fischer}@LNT.de

Thorsten Wild, Cornelis Hoek
Alcatel-Lucent Deutschland AG
Bell Labs Germany
Physical Layer Solutions, ZFZ/R
Lorenzstraße 10, 70435 Stuttgart

***Abstract*—The effects of cooperating base stations in the downlink of an OFDM-based cellular network with frequency reuse factor one are studied. In this so-called network MIMO scenario the signals of several users are jointly processed before transmission in order to handle the unavoidable multi-user interference. We apply and study pre-processing techniques well-known from conventional MIMO scenarios in the network environment. Tomlinson-Harashima precoding offers a variety of beneficial characteristics in this setting. In terms of the achievable link capacities it outperforms linear pre-processing approaches.**

I. Introduction

In future mobile communication systems ("beyond LTE" or 4G) *orthogonal frequency-division multiplexing (OFDM)* [4] in combination with *frequency-division duplex (FDD)* is most likely used to manage the dispersive radio channels and to separate up- and downlink, respectively. To increase the spectral efficiency and hence the data rate of the systems and to enhance the reliability of transmission, multiple-input/multiple-output (MIMO) techniques have to be introduced. Furthermore, network providers strongly urge for a frequency reuse factor of one. These measures result in severe multi-user respectively multi-antenna interference on the received signals. In order to avoid limitations of the network performance, these interferences have to be compensated for.

Considering coming cellular networks, the MIMO character of the system is not necessarily constituted by the use of dedicated antenna arrays at transmitters and/or receivers, but the individual base stations of different cells or sectors also form parts of an even larger MIMO system. A so-called "distributed MIMO" or "network MIMO" scenario is present, in which the sensible coordination and cooperation of adjacent base stations is one of the main challenges. Regarding for example the downlink of a network MIMO scenario, the signals of several base stations can be jointly processed to provide the spatially scattered users with their non-interfered signals. Ideally, all base stations have to be perfectly synchronized and have to have knowledge of the entire propagation scenario to achieve this goal. From a practical point of view this is infeasible and only spatially limited cooperations can be pursued.

In this paper, we assess approaches realizing varying stages of cooperation in the downlink transmission of a cellular network, i.e., we include varying numbers of surrounding base stations into the cooperation. The general potentials of a joint pre-processing in network MIMO scenarios are analyzed to identify a reasonable but still manageable degree of cooperation. The implementations of the pre-processing assessed in the network MIMO scenario are well-known from conventional MIMO scenarios: we employ linear pre-equalization and Tomlinson-Harashima precoding [6] or [11]. For the latter, two different applicable power allocation strategies are investigated. The individual approaches to network MIMO transmission are studied for varying degrees of cooperation using channel models familiar from the 3G standards [3]. We evaluate the performance results by means of the statistics of the individual link capacities in the network. The results of our analysis support a substantiated decision on the cooperation level in the network.

II. Network and System Model

We study *downlink OFDM transmission* in a cellular radio network, i.e., the communication of the base stations to the mobile terminals. The analysis of the network MIMO OFDM system is entirely performed in the frequency domain of the equivalent complex base band system [10]; a carrier frequency is not explicitly given.

We assume a regular hexagonal grid of N_{BS} base stations (BS) which carry $N_{\mathrm{S/BS}} = 3$ sector antennas each. To keep the problem manageable, each user equipment (UE) has just a single receive antenna. The user assignment in the network is strictly geometry-based, i.e., within each geometrically defined sector a single user can be served. In order to establish a network MIMO system, we assume that the signals of N_{S} (adjacent) sectors serving (at most) N_{S} users can be jointly processed before transmission.[1] Non-cooperating base stations act as interferers in this scenario. In the following, we enumerate the cooperating sector antennas with the index $\mu = 1, \dots N_{\mathrm{S}}$, the users served by the cooperating sector antennas with the index $\nu = 1, \dots, N_{\mathrm{S}}$.

In order to model the links between each sector antenna and user equipment, we use a discrete-time channel model (on time-domain symbol raster of discrete time T_{c}) comprising pulse shaping at the transmitter, the continuous time dispersive channel, matched filtering, and sampling in time domain. Applying the well-known components of standard OFDM transmission (inverse discrete Fourier transform (DFT), guard interval insertion, guard interval removal, and DFT) to each channel individually, we obtain a set of D decoupled parallel subchannels in frequency domain. These are described by complex transfer coefficients which in the d-th carrier

[1] For convenience, the number of served users here equals the number of transmit antennas.

($d = 1, \ldots, D$) and for the link from BS μ to UE ν reads

$$h_{\nu,\mu}^{(d)} = \sum_k h_{\nu,\mu}[k]\, \mathrm{e}^{-\mathrm{j}2\pi k(d-1)/D} \,. \tag{1}$$

Here, $h_{\nu,\mu}[k]$ denotes the respective discrete time channel impulse response. For the description of the MIMO channel experienced in the d-th carrier, we use the $(N_\mathrm{S} \times N_\mathrm{S})$-*channel matrix*

$$\boldsymbol{H}^{(d)} \stackrel{\text{def}}{=} \left[h_{\nu,\mu}^{(d)} \right]_{\substack{\nu=1,\ldots,N_\mathrm{S} \\ \mu=1,\ldots,N_\mathrm{S}}} \,. \tag{2}$$

At the transmitter side, we denote the data symbols designated for the ν-th user in carrier d as $a_\nu^{(d)}$. The channel symbols $x_\mu^{(d)}$ actually radiated from the μ-th transmit antenna are generated from the initial data symbols by some kind of pre-processing still to be specified. At the receiver, the symbols of the ν-th user equipment are denoted as $y_\nu^{(d)}$. Using vector-matrix notation frequency-domain receive signals in the d-th carrier compute to

$$\boldsymbol{y}^{(d)} = \boldsymbol{H}^{(d)} \boldsymbol{x}^{(d)} + \boldsymbol{n}^{(d)} \,. \tag{3}$$

Note, here $\boldsymbol{y}^{(d)}$ and $\boldsymbol{x}^{(d)}$ are N_S-dimensional column vectors containing the respective signals for the d-th carrier. The vector $\boldsymbol{n}^{(d)}$ represents the N_S additive white Gaussian noise terms with variance σ_N^2 imposed onto the received signals.

Obviously, the interference of non-cooperating users has been neglected in (3). In order to reflect the interference of the $N_\mathrm{BS} N_\mathrm{S/BS} - N_\mathrm{S}$ sectors/users not included in the joint signal processing, we introduce an interference term $\boldsymbol{s}^{(d)}$ and obtain

$$\boldsymbol{y}^{(d)} = \boldsymbol{H}^{(d)} \boldsymbol{x}^{(d)} + \boldsymbol{n}^{(d)} + \boldsymbol{s}^{(d)} \,. \tag{4}$$

We define a signal-to-noise ratio (SNR) E_s/N_0 where E_s is the average energy per channel symbol *at the transmitter side* $E_\mathrm{s} = \sigma_X^2 \cdot T_\mathrm{c}$, and σ_X^2 is the variance of the (zero-mean) channel symbols. The one-sided noise power spectral density *at the receiver input* is denoted by N_0 and related to the noise variance at the receiver by $N_0 = \sigma_\mathrm{N}^2 \cdot T_\mathrm{c}$.

For the evaluation of the system's performance we additionally define a user-related carrier-to-interference (CIR) ratio, which for the non-cooperating case reads

$$(C/I)_\nu^{(d)} = \frac{|h_{\nu,\nu}^{(d)}|^2 E_\mathrm{s}}{N_0 + \sigma_S^2} \,, \tag{5}$$

where the term σ_S^2 represents the entire (residual) multi-antenna interference imposed onto the receive signal of user ν. Thus, this term varies with the degree of cooperation achieved in the system. Finally, the CIR is then used to determine the link capacity (in bots per second) for the ν-th user

$$\mathsf{C}_\nu = \sum_{d \in D_\mathrm{used}} \Delta f \log_2 \left(1 + (C/I)_\nu^{(d)} \right) \,. \tag{6}$$

Here, Δf denotes the sub-carrier spacing and D_used is the set of actually used carriers.

III. MIMO Pre-Processing

Before we turn to network MIMO scenarios, we first briefly revisit the MIMO pre-processing techniques we later want to assess in this environment. The starting point for this short review is a conventional $N_\mathrm{S} \times N_\mathrm{S}$ MIMO system as it is formally described by (3), where a joint processing of the signals at the transmitter side is feasible. The techniques discussed below are applied per carrier in the MIMO OFDM system. Consequently, we focus on a single one of the D carriers in this section; the index d is dropped for convenience.

A. Linear Pre-Equalization

The first approach to handle the multi-antenna interference in a MIMO system and to decouple the spatial data streams is the simple inversion of the channel matrix $\boldsymbol{H}$, i.e., $\boldsymbol{F} = \boldsymbol{H}^{-1}$ is applied to the vector of data symbols before transmission (aka. zero-forcing linear pre-equalization, see Fig. 1 for a respective block diagram)

$$\boldsymbol{x} = \lambda \boldsymbol{F} \boldsymbol{a} \,. \tag{7}$$

In order to prevent a power amplification, the transmit signal is scaled by a factor λ, i.e., $\sigma_X^2 = \sigma_A^2$ is ensured. The scaling factor is given by

$$\lambda = \sqrt{\frac{N_\mathrm{S}}{\mathrm{trace}\left(\boldsymbol{F} \boldsymbol{F}^\mathsf{H} \right)}} \,. \tag{8}$$

Note, the individual transmit powers of the antenna signals may significantly vary in this approach; the sum power emitted by the N_S transmit antennas is constant, though. We later refer to this power allocation strategy as *sum power constraint*.

At the receiver side, in each user equipment only the scaling by λ has to be compensated for (multiplication with $\gamma = 1/\lambda$). The multi-antenna interference due to the $N_\mathrm{S} - 1$ other users in the MIMO system is completely suppressed, the signal of user ν only suffers from the (scaled) thermal noise.

B. Tomlinson-Harashima Precoding

Tomlinson-Harashima precoding initially was introduced for transmission over single-input/single-output frequency-selective channels [9], [7] and later extended to MIMO transmission [12], [6]. THP is the most simple realization of Costa's *writing on dirty paper* concept [5] and can be interpreted as the transmitter side dual to (spatial) decision-feedback equalization (DFE).

The transmitter consists of a permutation matrix $\boldsymbol{P}$, anon-linear feedback loop with lower triangular, unit main diagonal matrix $\boldsymbol{B}$, modulo reduction to the support of the respective signal constellation, diagonal gain matrix $\boldsymbol{\Lambda}$, and unitary feedforward matrix $\boldsymbol{F}$ (see Fig. 2 for a block diagram). At the receivers the signals have to be individually scaled with factors γ_ν (collected in a diagonal matrix $\boldsymbol{\Gamma}$) and the following processing (decision device or bit metric computation) has to take the modulo congruence of the signal points into account. The matrices have to fulfill

$$\boldsymbol{\Gamma} \boldsymbol{H} = \boldsymbol{P}^\mathsf{T} \boldsymbol{B} \boldsymbol{\Lambda}^{-1} \boldsymbol{F}^{-1} \,. \tag{9}$$

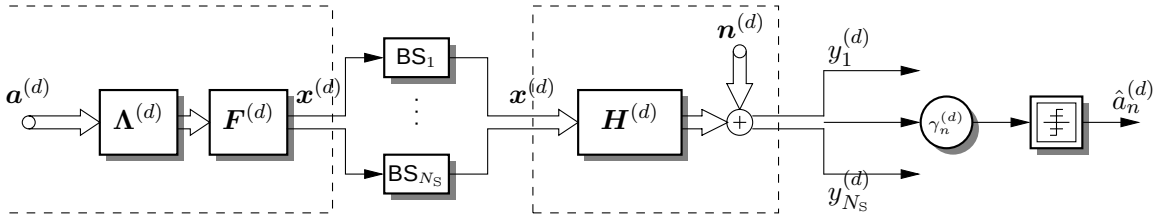

Fig. 1. Block diagram of (zero-forcing) linear pre-equalization. Situation shown for d-th carrier of MIMO OFDM system.

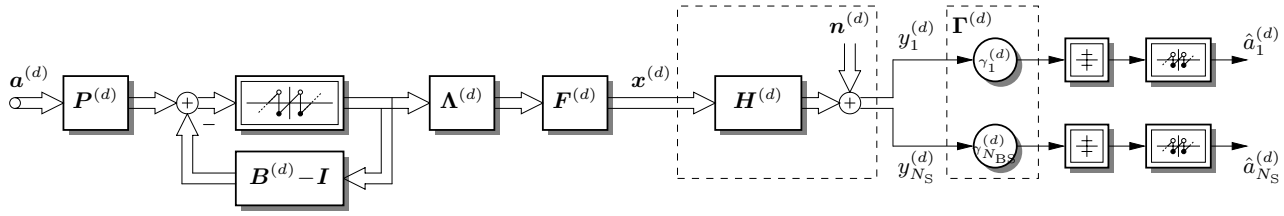

Fig. 2. Block digram of Tomlinson-Harashima precoding. Situation shown for d-th carrier of MIMO OFDM system.

For a detailed description of the computation of these matrices we refer to [11]. Using THP, the succession of the users in the pre-processing determined by $\boldsymbol{P}$ can be exploited for optimizations. Here, in these considerations, we focus on the zero-forcing variants of THP.

1) Sum Power Constraint: For THP we can easily pursue two different power allocation strategies. First, we can aim at an unchanged sum power, as we suggested for linear pre-equalization in Section III-A. In this case, the transmitter side diagonal scaling matrix computes to

$$\boldsymbol{\Lambda} = \frac{1}{\gamma} \boldsymbol{F}^{\mathsf{H}} \boldsymbol{H}^{-1} \boldsymbol{B}\,, \tag{10}$$

where γ is a scaling factor given by

$$\gamma = \sqrt{\mathrm{trace}\left(\left(\boldsymbol{F}^{\mathsf{H}} \boldsymbol{H}^{-1} \boldsymbol{B}\right)^2\right)}\,. \tag{11}$$

At the receiver side only a global scaling factor γ has to be compensated for.

2) Per-Antenna Power Constraint: The second power allocation strategy applicable to THP is a *per-antenna power constraint*, i.e., the individual transmit powers are identical to those of non-pre-processed transmission. To achieve this goal, the transmitter side diagonal scaling matrix has to be chosen as the identity matrix, i.e., $\boldsymbol{\Lambda} = \boldsymbol{I}$. At the receivers, the individual scaling factors γ_ν of the users may vary and comprised in a diagonal matrix are obtained by

$$\boldsymbol{\Gamma} = \boldsymbol{B} \boldsymbol{F}^{\mathsf{H}} \boldsymbol{H}^{-1}\,. \tag{12}$$

As the scaling factors usually differ, so do the individual CIRs and link capacities. An optimization of the permuation matrix $\boldsymbol{P}$ may lead to enhanced the link capacities.

Note, the per-antenna power constraint could also be applied to linear pre-equalization. The derivation of the respective scaling factors is complicated and based on numerical optimization in this case, cf. [8]. We therefore omit this approach.

IV. Network MIMO

Turning now to network MIMO OFDM systems, we first discuss several different approaches to base station cooperation. Afterwards, the link capacities of the individual realizations of network MIMO are assessed.

A. Network Cooperation Settings

The cooperation of several sectors/base stations in the network is based on the assumption, that all of the participating transmitters are linked with a central processing unit via a powerful backbone network to exchange both, the actual transmit signals and the side information required for the coordinated transmission. Especially the latter may represent a non-trivial part for the amount of channel state information needed to appropriately pre-process the signals is non-negligible. Here, in this context, we focus on theoretically achievable advantages of cooperating base stations. The related unavoidable efforts in the network are neglected. In the following, we introduce three different approaches to coordinated transmission in the network. Fig. 3 illustrates these settings. To cover the entirearea of the network, the proposed approaches have to be periodically repeated.

1) Cooperation at a Single Base Station: First, we consider an approach which has some undeniable advantages over the other two attempts in terms of complexity. Consider a base station which is assumed to carry $N_{\mathrm{S/BS}} = 3$ sectorized transmit antennas, i.e., each antenna is intended to cover a sector of $120°$. Taking into account the non-ideal patterns of the employed antennas (cf. e.g. [3]), one can easily recognize the interference situation to handle even for a single isolated base station. Coordinating the three sectors and pre-processing the signals of the respective users is rather simple here, as the central processing unit can be incorporated into the base station itself. The MIMO system established by this approach is rather small in dimensions (3×3). The advantages of this kind of cooperation for users located at the far borders of the served sectors are questionable, though.

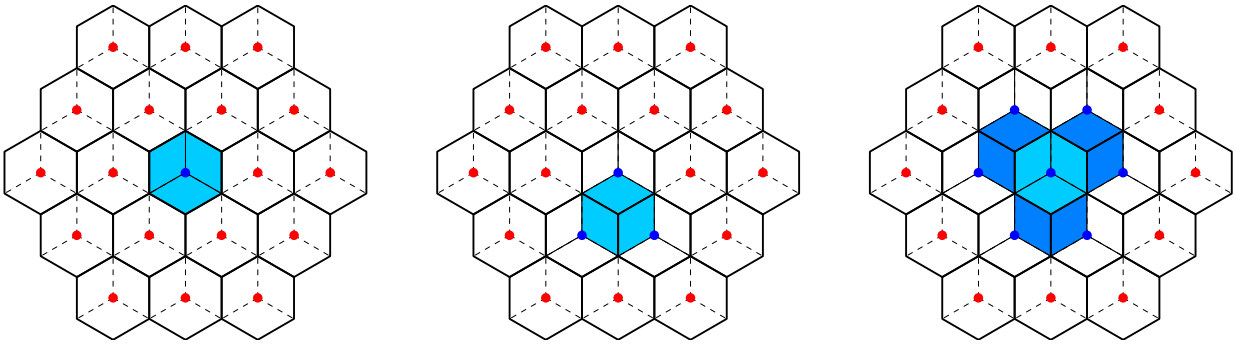

Fig. 3. Hexagonal grid structure of the scenario with cooperation at a single BS (left), with cooperation of three sectors of three BSs (center), and cooperation of nine sectors of seven BSs (right). Situation shown for 3-tier cluster with one central BS, 6 BSs at first tier, and 12 BSs at second tier ($N_{\mathrm{total}} = 37$). Area of UEs included in coordination in shades of blue; identical characteristics indicated by equal shades.

2) Three Cooperating Base Stations: Next, we again consider three coordinated sectors now belonging to three different base stations (cf. center plot of Fig. 3). This setting also provides an improvement of the interference situation at the far borders of the sectors where in an uncoordinated network usually the worst CIRs are expected. For the cooperation of these three sectors now a central processing unit managing the signals and channel state information is required. Compared to the non-coordinated case, this concept offers—beyond the interference cancellation—an increased degree of freedom for the admissible positions of the three users. They can move within the entire region covered by the three coordinated sectors and are not restricted to their geometrically determined sector. As for the cooperation addressed in Section IV-A1, we obtain a simple 3×3 MIMO system. This keeps the required matrices at a manageable size.

3) Seven Cooperating Base Stations: In order to evaluate potential advantages of a cooperation exceeding three sectors, we investigate a scenario where nine sectors of seven adjacent base stations are coordinated (cf. right plot of Fig. 3. This can be also understood as a mixture of the first two approaches: the three sectors of the inner base station and the inward-oriented sectors of the base stations located at the next tier are coordinated. The resulting 9×9 MIMO system might be a challenge for the online computation of the required matrices, though. Furthermore, the overhead of side information required for the pre-processing is significantly increased.

Extending the cooperation in the network to even larger dimensions reinforces these effects and thus is not investigated here. Taking into account a realistic path loss of the signals (cf. Tab I), the attenuation of these potential interferers may be tremendous and their contribution to the interference insignificant.

B. Performance Evaluation

In order to qualitatively assess the performance of the different cooperation strategies and pre-processing techniques, the respective scenarios were simulated for a network MIMO OFDM setting.

1) General Comparison: First, we briefly compare the proposed power allocation approaches and the situation of the residual interference.

The sum power constraint offers more degrees of freedom as only the sum power radiated via the N_{S} transmit antennas has to be meet a constraint. The individual transmit powers can be adapted according to some criterion. For both, linear pre-equalization and THP in this case the goal is to equalize the users' receiver side signal-to-noise ratios. In terms of fairness this approach is optimal. The per-antenna power constraint in contrast is more strict and clearly demands the individual transmit powers to be identical. Obviously, this results in varying receiver side SNRs of the users.

From (6) it can be seen that the residual interference imposed onto the receive signal affects the CIR. In the first two proposed cooperation approaches each user experiences similar residual interference. The cooperation suggested in IV-A3 leads to inconsistent interference situations. Users located in the inner part of the region covered by the nine sectors obviously suffer from less residual interference as do the users positioned in the outer sectors. Thus, the individual link capacities may vary in this case.

2) Numerical Results: Finally, we present numerical results for the link capacities. The simulations were based on parameters for the transmission system closely following [1], i.e., the OFDM system has $D = 256$ carriers wherefrom $D_{\mathrm{used}} = 151$ are used; a subcarrier spacing of $\Delta f = 15$ kHz and a signal bandwidth of $B = 2.5$ MHz. The antenna pattern was chosen according to [3]. Furthermore, we used a wide-sense stationary uncorrelated scattering channel model with parameters as summarized in Tab I.

TABLE I
PARAMETERS OF THE CHANNEL MODEL (CF. [1], [2]).

Power-delay profile	following "Pedestrian B" model
Number of taps	6
Path loss	according to [1, Tab. A.2.1.1-3]
	$\mathrm{PL}\ [\mathrm{dB}] = -(128.1 + 37.6 \log_{10}(w\ [\mathrm{km}]))$
Shadowing	according to [1, Tab. A.2.1.1-3]
	log-normal distributed with 8 dB std. dev.

In Fig. 4 the average capacities of the different approaches are given over the position in the region covered by the cooperating sectors. Averaging was performed over numerous channel realizations and various positions of the coordinated

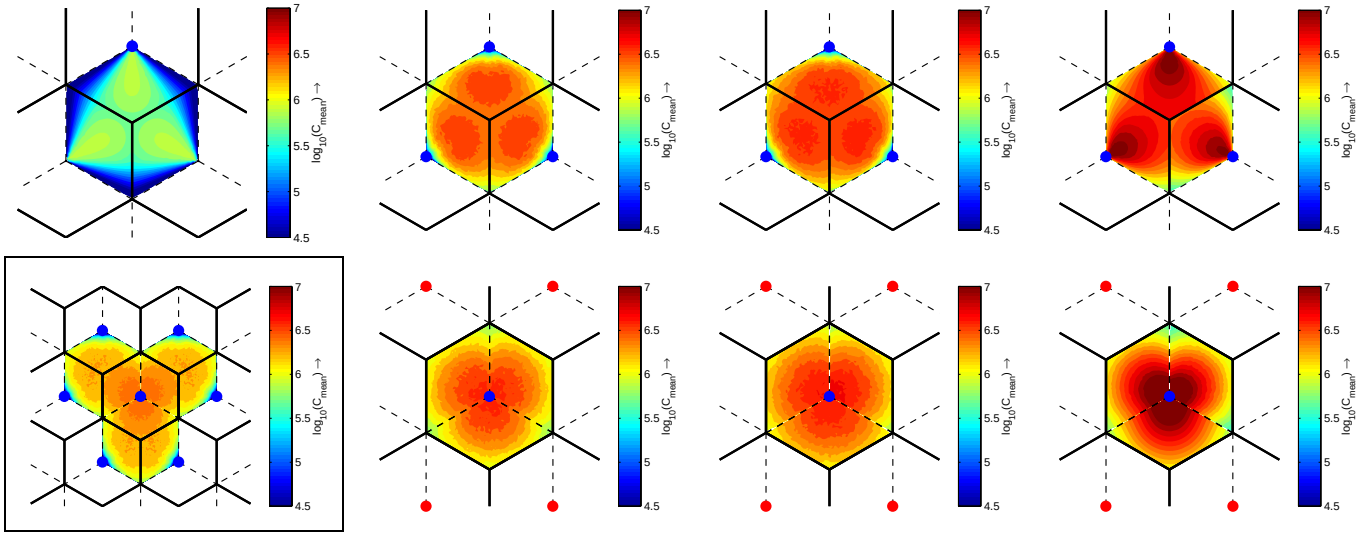

Fig. 4. Average capacities C_ν of users $\nu = 1, \ldots, N_\mathrm{S}$ over position in network in bits per second. Top left: situation without cooperation. Rest of top row: coordination of $N_\mathrm{S} = 3$ adjacent sectors of $N_\mathrm{BS} = 3$ base stations. Bottom left: coordination of $N_\mathrm{S} = 9$ sectors of seven base stations with linear pre-equalization. Rest of bottom row: coordination of $N_\mathrm{S} = 3$ sectors of a single base station. Second column: linear pre-equalization; third column: THP with sum power constraint. Right-most column: THP with per-antenna power constraint. $E_\mathrm{s}/N_0 \mathrel{\widehat{=}} 120$ dB; consideration of 2 tiers.

users. The top row shows the results for three coordinated sectors of three adjacent base stations (cf. Sec. IV-A2) and a non-coordinated scenario for comparison (left-most plot). The advantages of coordination can be clearly recognized, as can be the slight superiority of THP over linear pre-equalization. For the THP approaches the per-antenna power constraint leads to capacities stronger varying with the position of the user in the sector. The capacity obtained by the the sum power constraint is mostly outperformed by the per-antenna power constraint. The first, however, equalizes the link capacities of the three users nearly independently of the position of their positions. The varying residual interference of non-coordinated sectors leads to slightly varying results (e.g., near the base stations due to interference of the other two sectors served by the very base station).

In the bottom row, the three right plots show the results for three coordinated sectors of single base station (cf. Sec. IV-A1). Again, we can observe significantly increased link capacities compared to the uncoordinated case. The advantages, however, are slightly less pronounced than those observed for the first 3×3 approach. Especially at positions far from any base station, the average capacities are rather low and loose due to the residual interference of non-cooperating adjacent sectors. Again, THP clearly outperforms linear pre-equalization. Using the per-antenna power constraint leads to extremer capacities, than does the sum power constraint.

The framed plot on the bottom left shows the results for a cooperation of nine sectors of seven base stations (cf. Sec. IV-A3). In this case only linear pre-equalization was simulated. As we can see, the gains due to coordination are not as distinct as they are for the 3×3 systems. Furthermore, we can observe an average link capacity which apparently varies with the position of the users. This results from the significantly changing residual interference situation within the region covered by the coordinated sectors. The inner users clearly benefit more than the users located in the outer sectors.

V. Conclusions

The results for the link capacity in the downlink of a network MIMO OFDM scenario show clear advantages of coordinated transmission even for a very limited number of participating sectors. Larger numbers of cooperating sectors do not enhance capacities. The per-antenna power constraint applicable with THP leads to on average overall increased capacities, whereas the sum power constraint bears the danger of transmit power wasted on the forced equalization of the users.

References

[1] 3GPP technical specification group radio access network; physical layer aspect for evolved universal terrestrial radio access (UTRA), 2006.

[2] 3GPP technical specification group radio access network; radio frequency (RF) system scenarios, 2007.

[3] 3GPP technical specification group radio access network; spatial channel model for multiple input multiple output (MIMO) simulations, 2007.

[4] J. A. C. Bingham. Multicarrier modulation for data transmission: An idea whose time has come. *IEEE Comm. Mag.*, 28(5):5–14, May 1990.

[5] M. H. M. Costa. Writing on dirty paper. *IEEE Trans. on Information Theory*, 29(3):439–441, May 1983.

[6] R. F. H. Fischer, C. Windpassinger, A. Lampe, and J. B. Huber. Space-time transmission using Tomlinson-Harashima precoding. In *Proceedings 4. ITG Conference on Source and Channel Coding*, pages 139–147, Berlin, Germany, Jan. 2002.

[7] H. Harashima and H. Miyakawa. Matched-transmission technique for channels with intersymbol interference. *IEEE Trans. on Comm.*, 20(4):774–780, Aug. 1972.

[8] A. Tolli, M. Codreanu, and M. Juntti. Linear multiuser MIMO transceiver design with quality of service and per-antenna power constraints. *IEEE Trans. on Signal Processing*, 56(7):3049–3055, 2008.

[9] M. Tomlinson. New automatic equaliser employing modulo arithmetic. *IET Electronics Letters*, 7(5):138–139, Mar. 1971.

[10] H. L. V. Trees. *Detection, Estimation, and Modulation Theory*, volume III. John Wiley & Sons, New York, NY, USA, 2001.

[11] C. Windpassinger. *Detection and Precoding for Multiple Input Multiple Output Channels*. PhD thesis, Friedrich-Alexander-Universität Erlangen-Nürnberg, 2004.

[12] C. Windpassinger, R. F. H. Fischer, T. Vencel, and J. B. Huber. Precoding in multi-antenna and multi-user communications. *IEEE Trans. on Wireless Comm.*, 3(4):1305–1316, July 2004.